

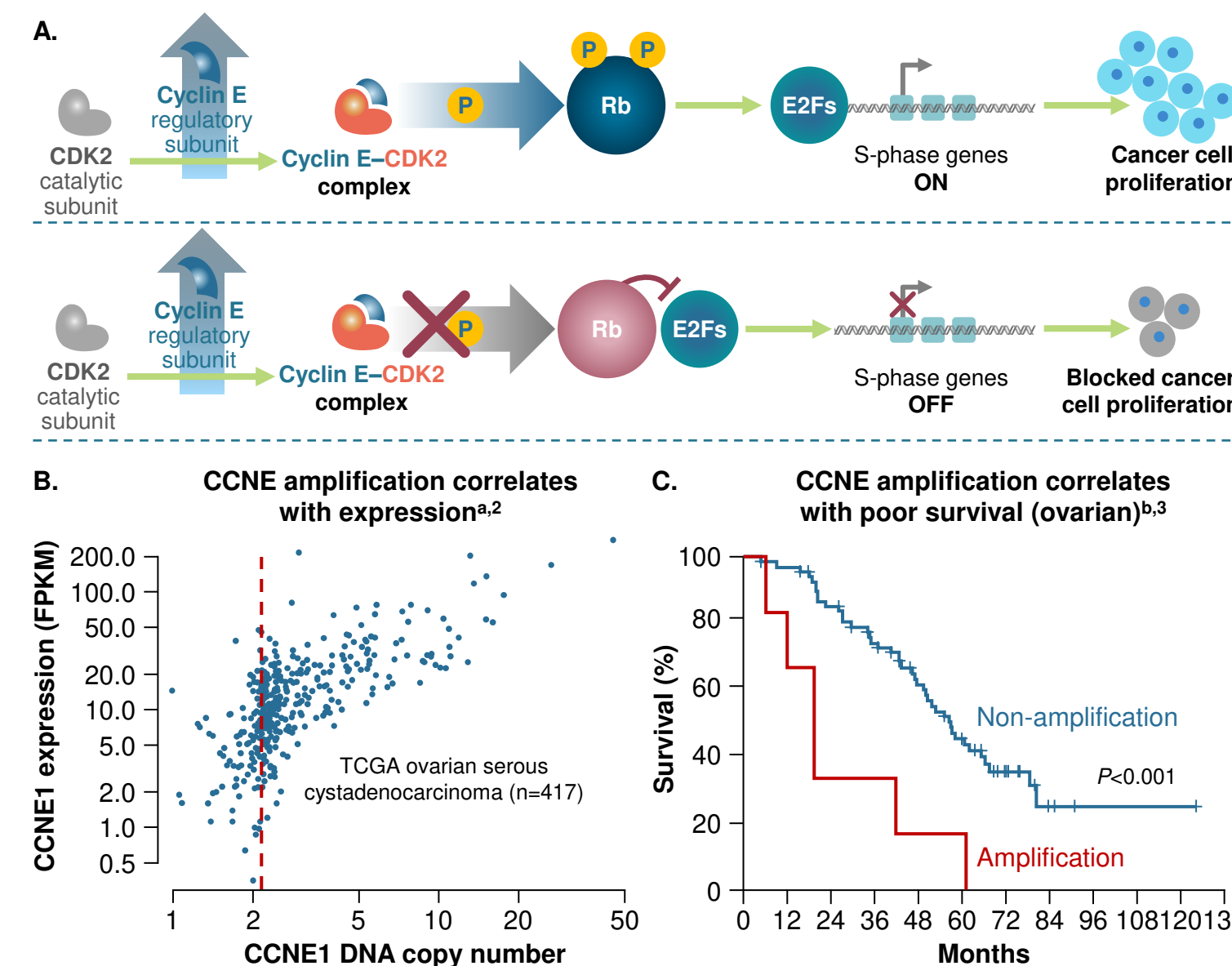
Yoon J. Choi¹, Steve Wenglowsky¹, Victoria Brown¹, Neil Bifulco¹, Yeon S. Choi¹, Jian Guo¹, Megan Hatlen¹, Joseph Kim¹, Tim LaBranche¹, Riadh Lobbardi¹, Emanuele Perola¹, Emily Rozsahegyi¹, Michelle Maynard¹, Phil Ramsden¹, Grace Silva¹, Faith Stevison¹, Richard Vargas¹, Ruduan Wang¹, Doug Wilson¹, Rich Woessner¹, Dean Zhang¹, Rob Meissner¹, Klaus Hoeflich¹, Marion Dorsch¹

¹Blueprint Medicines Corporation, Cambridge, Massachusetts, USA

Background

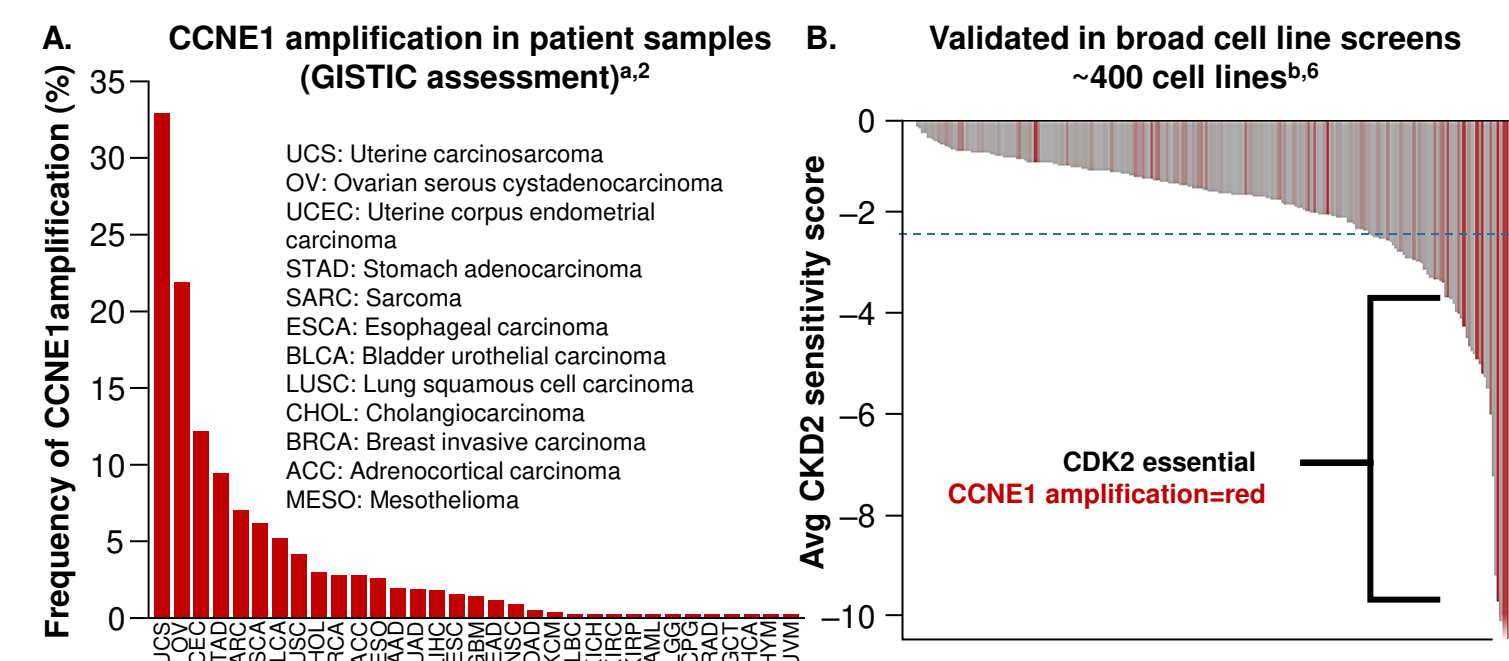
- Cyclin E1 and E2 are core cell cycle regulators, that when bound activate CDK2 (cyclin-dependent kinase 2), driving G1/S progression of the cell cycle¹ (Figure 1A)
- A broad range of aggressive cancers overexpress and/or harbor CCNE gene amplifications, thus CDK2 is a potentially important therapeutic target
 - In subsets of gynecological, breast, gastric, and other cancers, CCNE amplification correlates with overexpression (Figure 1B)² and has been associated with poor survival in ovarian cancer (Figure 1C)³
 - Cyclin E amplification/overexpression has been reported as a potential mechanism of resistance to CDK4/6 therapies in ER-positive HER2-negative breast cancer^{4,5}
- Deriving a highly selective CDK2 inhibitor, sparing CDK family members has been historically challenging; however, it is critical to limit off-target CDK-driven toxicities
- We report preclinical data supporting a potential best-in-class CDK2 inhibitor exhibiting single digit cellular nanomolar potency and selectivity against CDK 1, 4, 6, 7, 9 with single agent anti-tumor activity

Figure 1: Aberrant cyclin E levels inappropriately activate CDK2 and correlate with poor survival¹⁻³



E2F, transcription factor; FPKM, fragments per kilobase of transcript per million; P, phosphorylation; Rb, retinoblastoma protein; TCGA, The Cancer Genome Atlas. *The results shown here are in whole or part based upon data generated by the TCGA Research Network: <https://www.cancer.gov/tcga>. *Modified from Etamadmoghadam et al. 2019².

Figure 2: CCNE1 amplification across broad cancer types predicts response to CDK2 inhibition^{2,6}

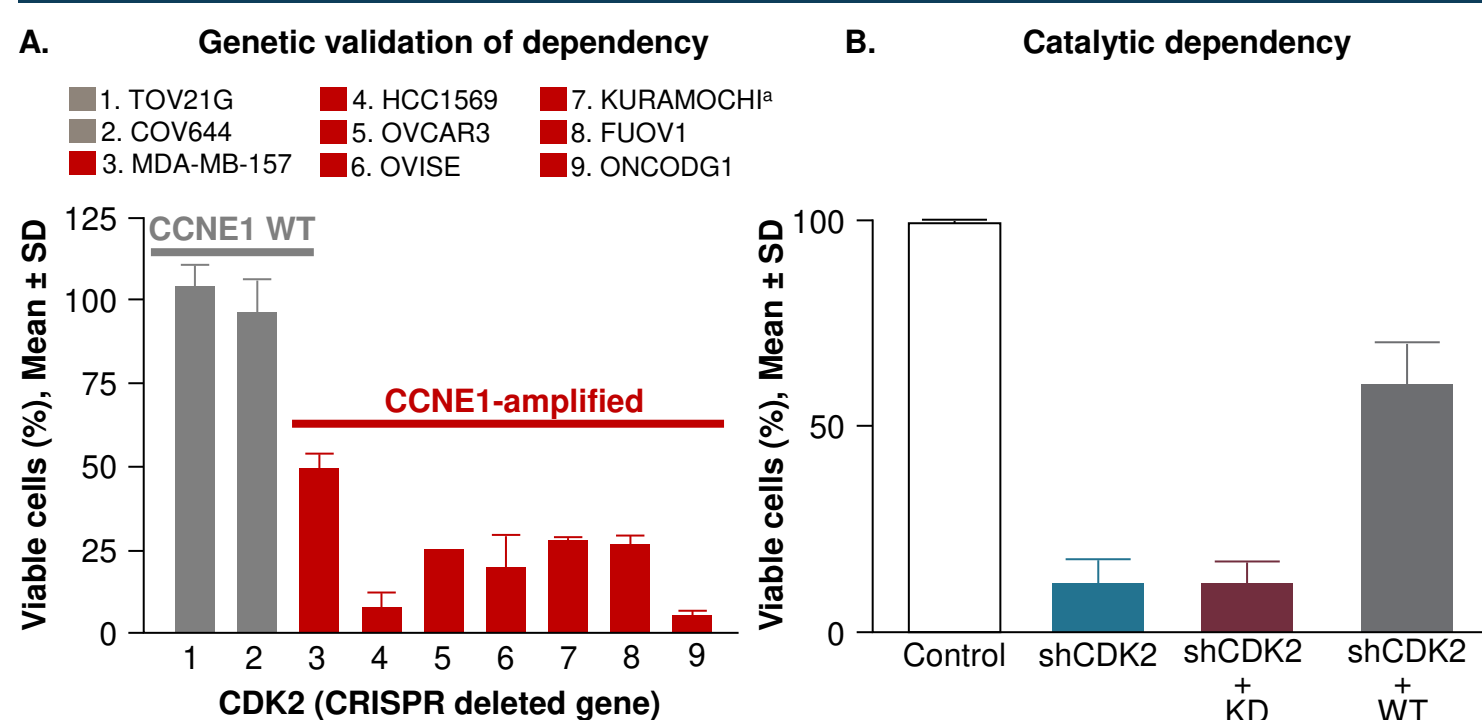


(A) CCNE1 GISTIC data across tumor types. CCNE1 amplification frequency represented as percentage of total patient samples. (B) CDK2 essentiality scores replotted from Project DRIVE. CCNE1-amplified cell lines (red bars) and non-amplified lines (gray bars) plotted against CDK2 essentiality score. Blue dotted line represents cut-off for essentiality.

GISTIC, Genomic Identification of Significant Targets in Cancer. *The results shown here are in whole or part based upon data generated by the TCGA Research Network: <https://www.cancer.gov/tcga>. *Modified Source data: McDonald et al. Project DRIVE, Cell 2017⁶.

Results

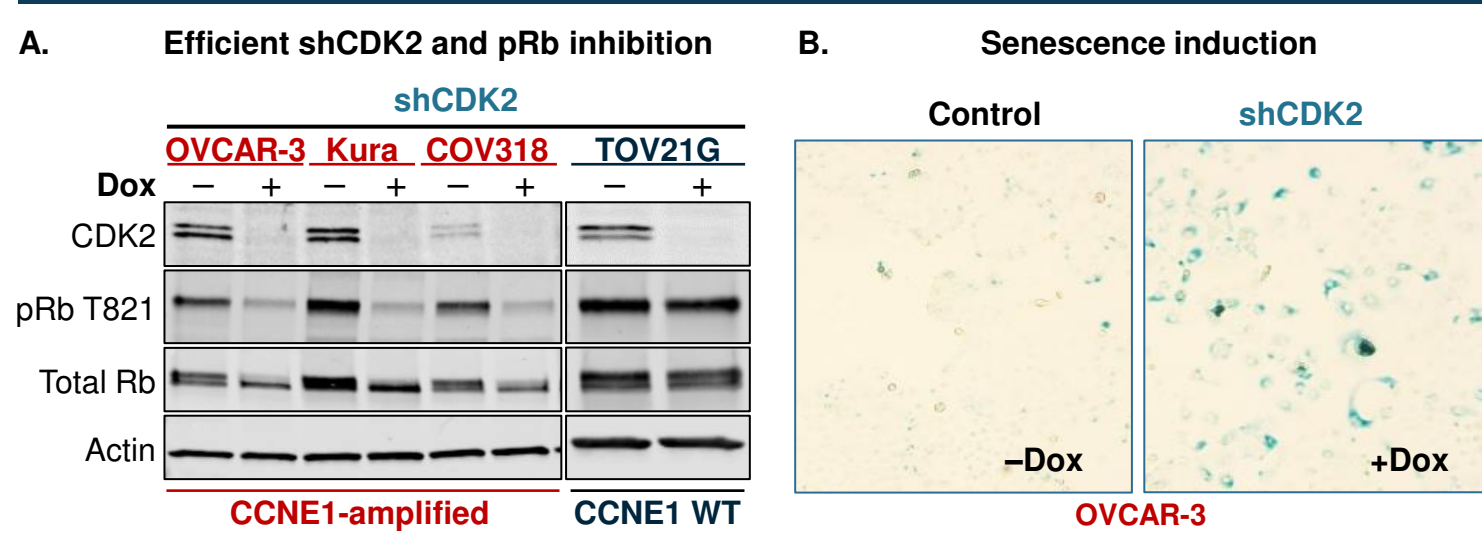
Figure 3: CDK2 catalytic activity is essential in CCNE1-amplified cell lines



(A) CRISPR screen in ovarian and breast cell lines. CDK2 was knocked-out in Cas9-expressing breast (3 and 4) and ovarian cell lines (1, 2, 5-9). The percentage of viable cells was determined after 21 days. (B) Proliferation in OVCAR-3 cells after CDK2 knockdown and rescue with WT or KD mutant CDK2. Empty vector, WT or T160A/D145N KD CDK2 was expressed in OVCAR-3 cells, followed by induction of CDK2-targeting shRNA. The percentage of growth is normalized to control at 14 days.

CRISPR, clustered regularly interspaced short palindromic repeats; KD, kinase dead; SD, standard deviation; shCDK2, shRNA against CDK2; sh, short hairpin; WT, wild-type (i.e., non-amplified/gain). *Kuramochi copy number gain.

Figure 4: CDK2 knockdown induces pRb inhibition and irreversible arrest in CCNE1-amplified cell lines



(A) Dox inducible knockdown of CDK2. Lysates were probed by Western blot as annotated. (B) SA-β-Gal staining in OVCAR-3 cells. Cells were treated with or without Dox for 6 days and stained SA-β-Gal. (C) Confluency after CDK2 knockdown. Cells were re-plated after 6 days of dox induction with or without sustained knockdown (+/- dox).

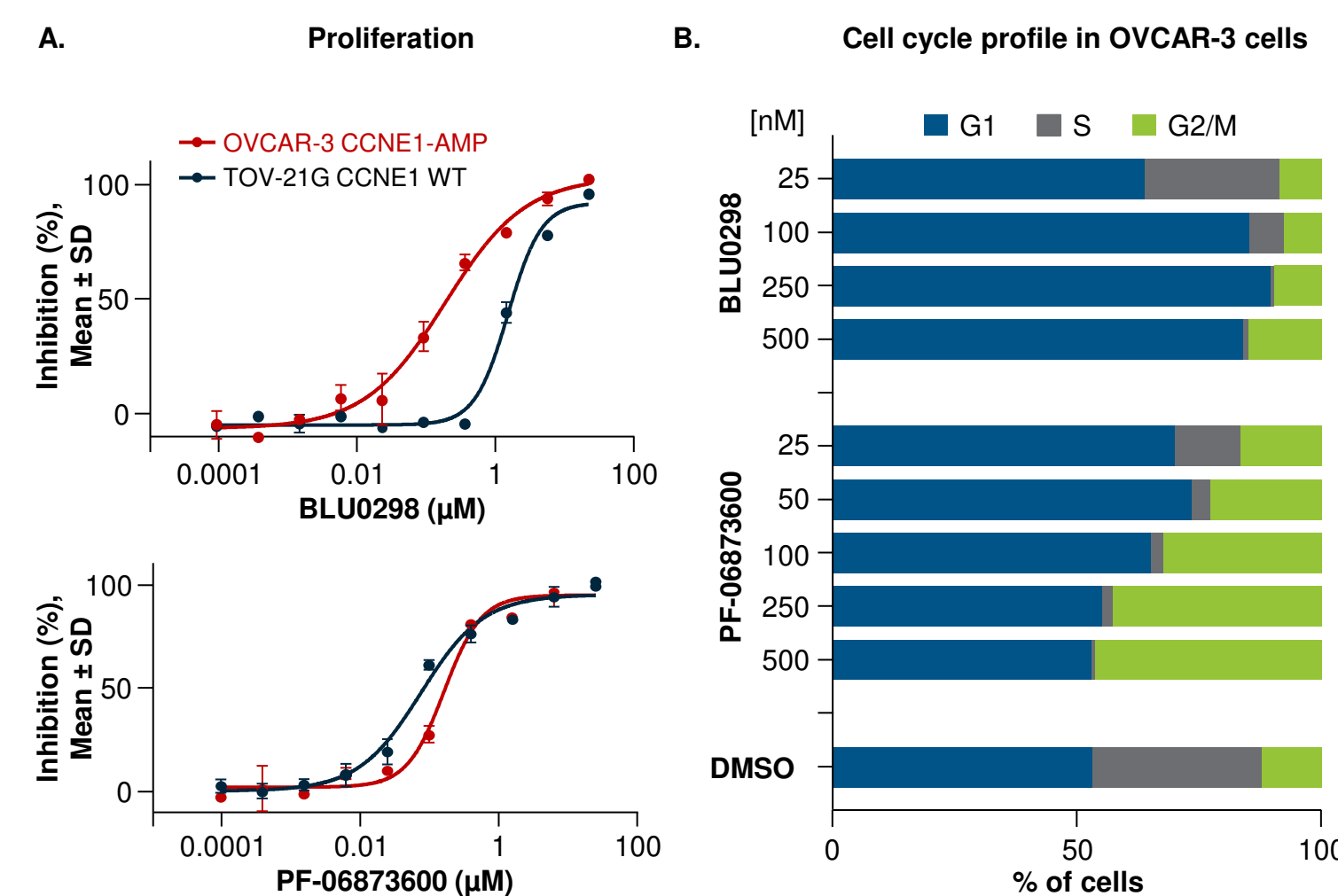
Dox, doxycycline; KD, knockdown; SD, standard deviation; WT, wild-type (i.e., non-amplified).

Table 1: BLU0298, BLU1954, and BLU2256 are selective, potent CDK2 inhibitors sparing CDK off-targets including CDK1

Compound	Kinome S (10) ^a	pRb (CDK2 cell)	p"X" (CDK1 cell)	Cellular activity IC ₅₀ (nM) ^b							Enzyme activity IC ₅₀ (nM) ^c							
				CDK2	CDK1	CDK4	CDK6	CDK7	CDK9	CDK2	CDK1	CDK4	CDK6	CDK7	CDK9			
BLU0298	0.045	4.2	380.2	2.6	233.6	377.4	275.2	6941.2	6115.1									
BLU1954	0.055	1.6	127.7	0.2	110.1	114.5	190.6	3928.9	849.1									
BLU2256	0.040	2.6	133.7	0.1	152.9	116.9	393.2	4826.4	9063.2									
PF-06873600	0.094	1.9	42.8	0.4	31.8	1.5	5.7	3312.9	2481.1									

^aKinome S(10): fraction of kinases with <10 percentage of control at 3 μM among all the kinases tested, measured by KINOMEscan platform against 468 kinases. ^bpRb protein was assessed in synchronized OVCAR-3 cells to reflect CDK2 cellular potency; p"X" a validated CDK1 specific substrate was assessed in asynchronous OVCAR-3 cells. ^cEnzyme activities IC₅₀ were measured at 1 nM ATP using canonical CDK/Cyclin pairs: CDK2/Cyclin E1; CDK1/Cyclin B1; CDK4/Cyclin D1; CDK6/Cyclin D3; CDK7/Cyclin H1/MNAT1; CDK9/Cyclin T1. ATP, adenosine triphosphate; CDK, cyclin-dependent kinase; IC₅₀, half-maximal inhibitory concentration; pRb, phosphorylated retinoblastoma protein.

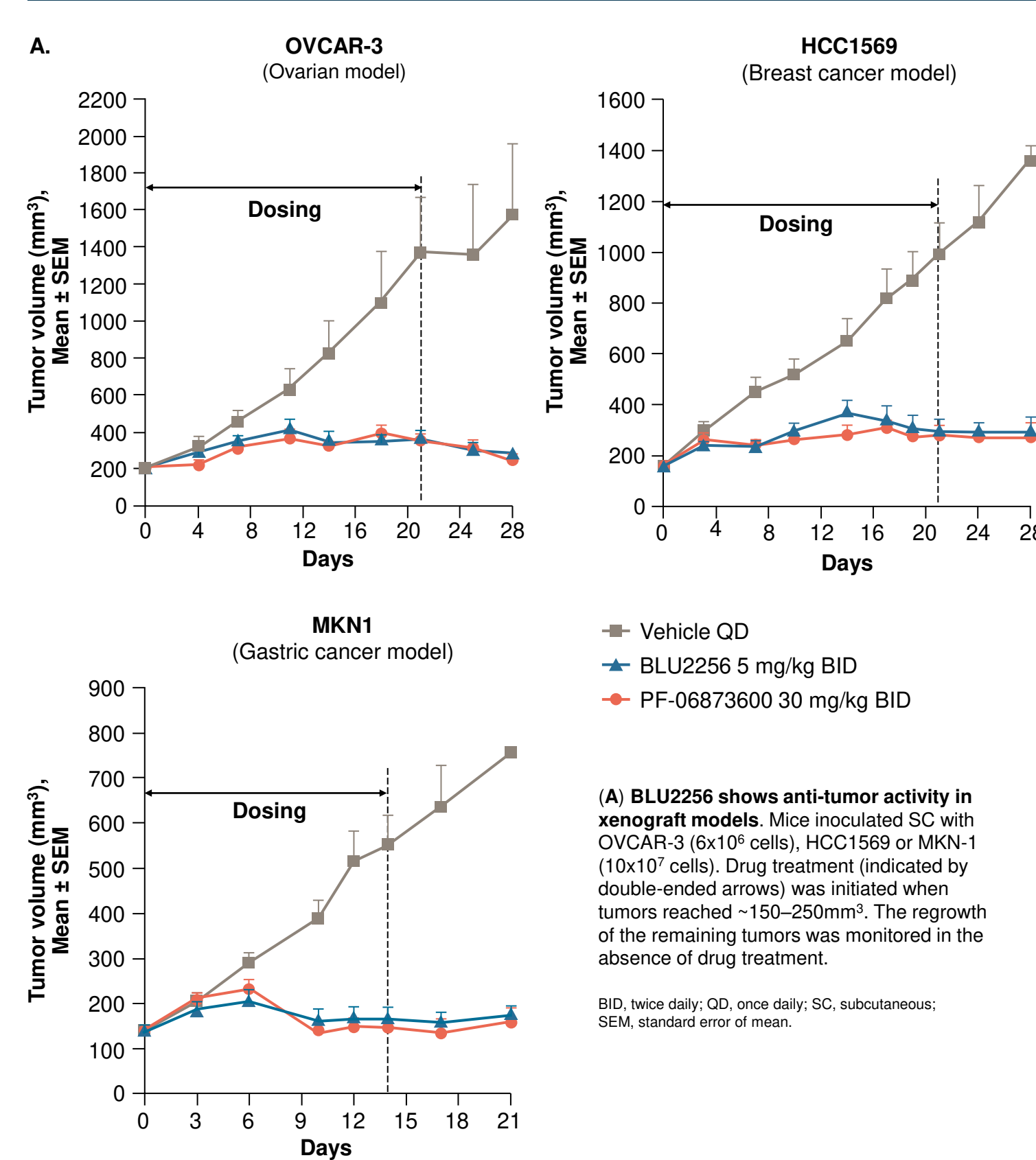
Figure 5: Selective CDK2 inhibitor, BLU0298 selectively inhibits (A) proliferation in CCNE1-amplified cells by (B) arresting cells in G1/S



(A) Dose response curves in ovarian cell lines. Ovarian cells were treated with BLU0298 or PF-06873600 for 5 days. Proliferation was assessed by CyQuant. (B) Cell cycle profile of OVCAR-3 cells. OVCAR-3 cells were treated with BLU0298 or PF-06873600 for 24 h. Cell cycle profile assessed by EdU incorporation (2 h) combined with DNA content (FxCycle).

DMSO, dimethyl sulfoxide; Dox, doxycycline; EdU, 5-ethynyl-2'-deoxyuridine; h, hour; SD, standard deviation; WT, wild-type (i.e., non-amplified).

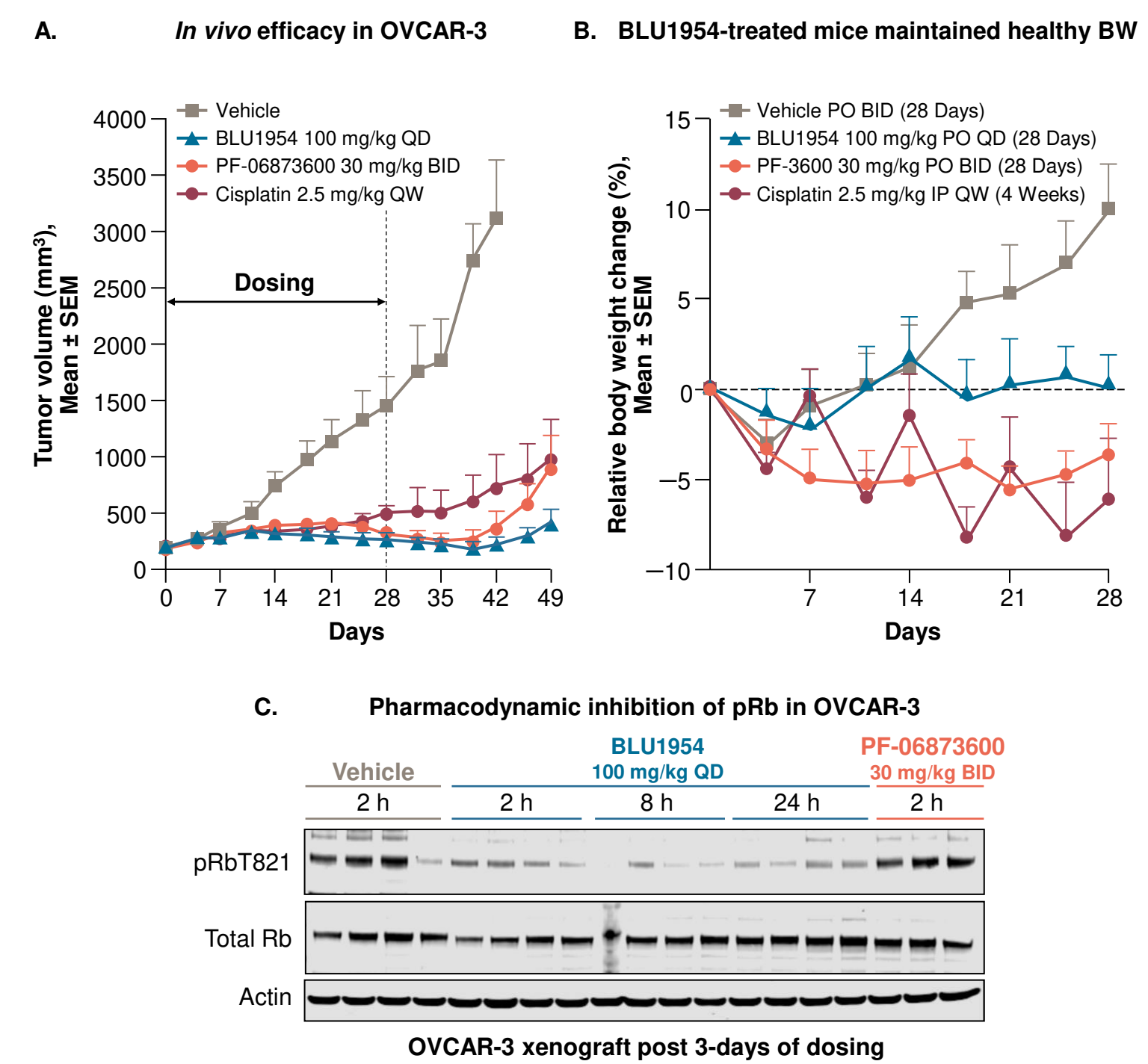
Figure 6: Selective CDK2 inhibition leads to sustained anti-tumor growth in CCNE1-amplified in vivo models



(A) BLU2256 shows anti-tumor activity in xenograft models. Mice inoculated SC with OVCAR-3 (6x10⁶ cells), HCC1569 or MKN-1 (10x10⁷ cells). Drug treatment (indicated by double-ended arrows) was initiated when tumors reached ~150-250mm³. The regrowth of the remaining tumors was monitored in the absence of drug treatment.

BID, twice daily; QD, once daily; SC, subcutaneous; SEM, standard error of mean.

Figure 7: Selective CDK2 inhibitor achieves similar efficacy to PF-06873600, a CDK2/4/6 inhibitor, or to chemotherapy, but maintains stable body weight



(A) Anti-tumor activity in OVCAR-3 xenograft. Mice were inoculated as in Figure 6. (B) Body weight measurement. Mice were monitored over 28 days and body weight measurements were taken twice a week. (C) Pharmacodynamic inhibition. Tumor lysates were assessed by Western blot at the indicated time points (vehicle, 2 h; BLU1954 2, 8, and 24 h; PF-06873600, 2 h) post 3-days of treatment.

BID, twice daily; BW, body weight; h, hour; IP, intraperitoneal; pRb, phosphorylated retinoblastoma protein; PO, orally; QD, once daily; QW, once a week; SEM, standard error of mean.

Conclusions and future directions

- Preclinical data indicate that aberrant CCNE is a predictor of response to CDK2 inhibition
- Targeting CDK2 in CCNE-aberrant cancer cell lines induces markers of senescence and irreversible arrest at G1/S
- BLU0298, BLU2256, and BLU1954 are selective, potent CDK2 compounds that lead to tumor growth inhibition
- CDK2 inhibitors show promise as monotherapy and are under evaluation in combination with CDK4/6 targeted therapies or chemotherapy
- Taken together these results provide scientific rationale for advancing this class of compounds toward clinical development in CCNE-aberrant cancers

References

- Malumbres M et al. *Genome Biol.* 2014;15:122. 2. TCGA Research Network: <https://www.cancer.gov/tcga>; last accessed March 23, 2021.
- Etamadmoghadam D et al. *PLoS One.* 2010; 5(11):e15498. 4. Knudsen ES et al. *ASCO Educational Book.* 2020;40:115-126. 5. Ding L et al. *Int J Mol Sci.* 2020;21:1960. 6. McDonald RE et al. *Cell* 2017;170:577-592.

Acknowledgments

Medical writing support was provided by Deborah Cantu, PhD, and editorial support was provided by Michelle Seddon, Dip Psych of Paragon, Knutsford, UK, supported by Blueprint Medicines Corporation, Cambridge, MA, according to Good Publication Practice guidelines.

Disclosures

This research was funded by Blueprint Medicines Corporation. Blueprint Medicines Corporation reviewed and provided feedback on the poster. The authors had full editorial control of the poster and provided their final approval of all content. YJC, SW, VB, NB, YSC, JC, JH, JK, TLB, RL, EP, ER, MM, PR, GS, FS, RV, RW, DW, RZ, DM, MD are employees of and hold equity interest in Blueprint Medicines Corporation. KH was an employee of Blueprint Medicines Corporation at the time of the work.